Supramolecular Association Between γ–Cyclodextrin and Preyssler-Type Polyoxotungstate

Nathalie Leclerc,[a]* Mohamed Haouas,[a] Clément Falaise,[a] Serge Al Bacha,[a,b] Loïc Assaud[b] and Emmanuel Cadot[a]

[a] *Institut Lavoisier de Versailles, UMR 8180 CNRS, UVSQ, Université Paris-Saclay, 78035 Versailles Cedex, France.*

[b] *Institut de Chimie Moléculaire et des Matériaux d'Orsay (ICMMO) – ERIEE, UMR 8182 CNRS, Université Paris-Saclay, 91400, Orsay, France.*

Supporting information

Table of Contents

1. FT-IR Spectra S2

2. Thermogravimetric analysis S3

3. Single crystal X-ray diffraction S4

3.1. Selected crystallographic parameters of the single-crystal X-ray diffraction structural analysis S4

3.2. Structural views of POM•1CD arrangement S5

4. NMR data S7

4.1. ^{1}H NMR titration S7

4.2. ^{31}P NMR S8

5. Electrochemical impedance spectroscopy S9

5.1. Warburg coefficient S9

5.2. EIS data S9

1. FT-IR Spectra

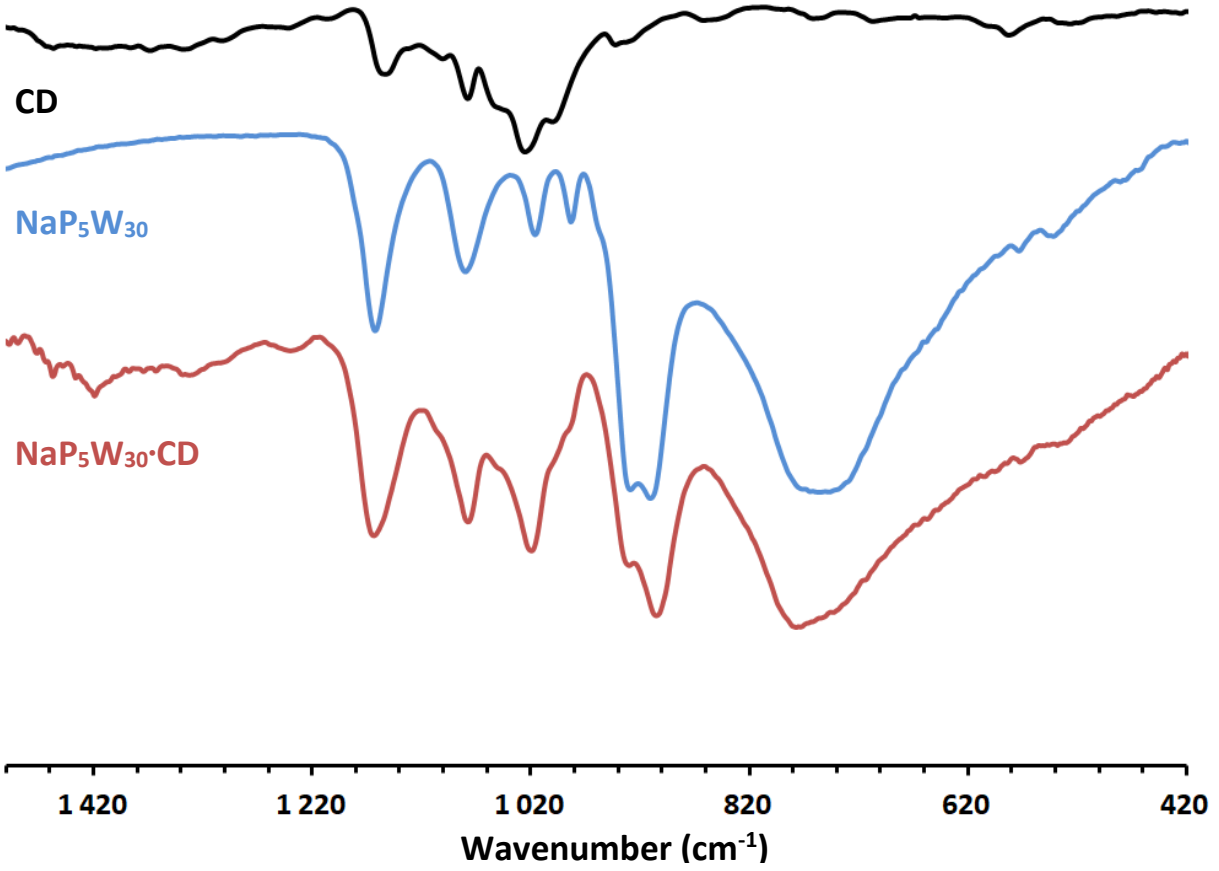

Figure S1. FT-IR spectrum of compound **NaP_5W_{30}•CD**, in comparison with the spectra of the precursor $K_{14}Na[P_5W_{30}O_{110}]$•$32H_2O$ (NaP_5W_{30}) and of the γ-cyclodextrin (CD). From NaP_5W_{30}•CD, the ratio of the bands of CD compared to that of the POM clearly increases (see the 1020 cm^{-1} band).

2. Thermogravimetric analysis

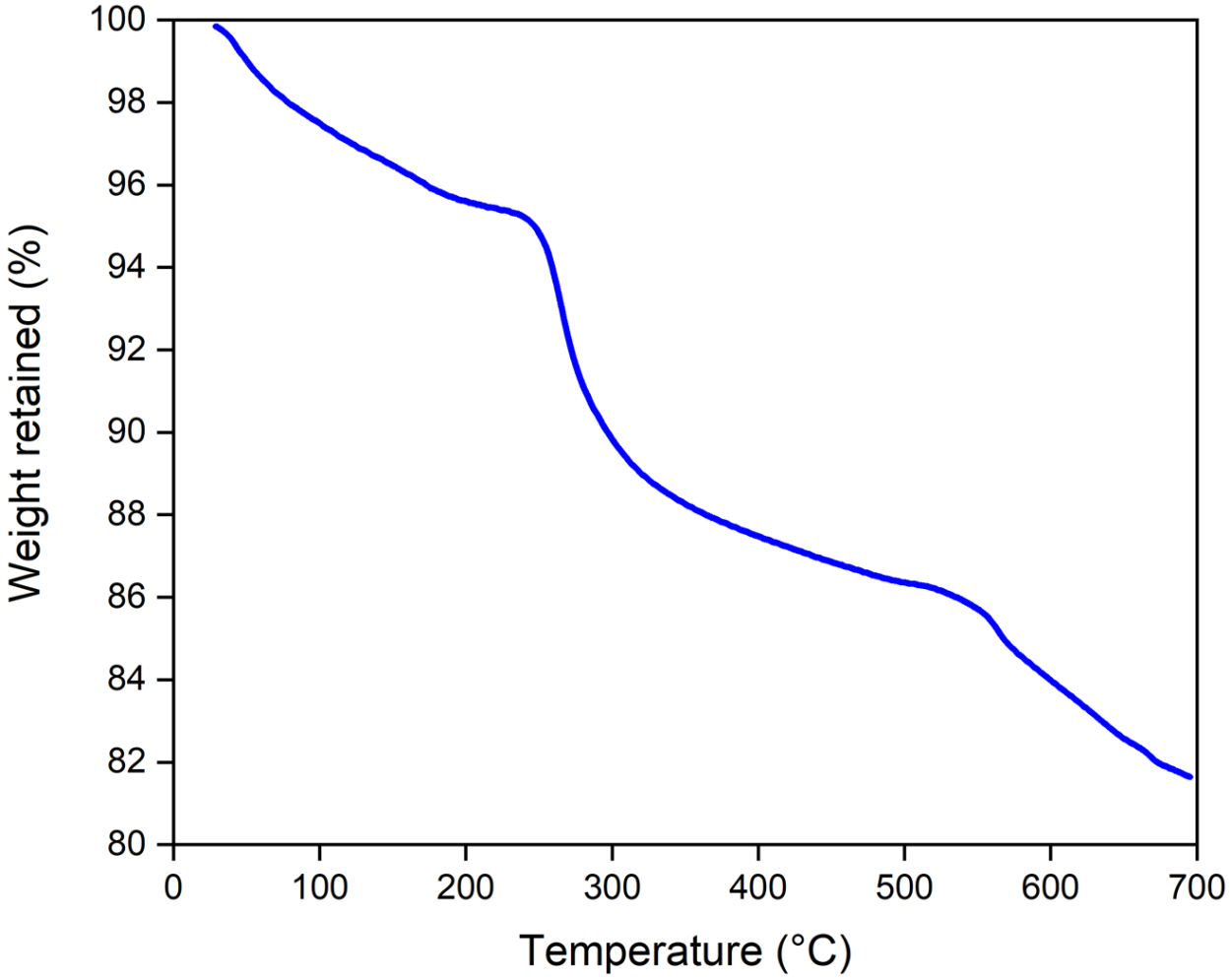

Figure S2. Thermogravimetric curve of freshly prepared **NaP_5W_{30}•CD**.

3. Single crystal X-ray diffraction

3.1. Selected crystallographic parameters of the single-crystal X-ray diffraction structural analysis

Table S1. Crystal data for NaP_5W_{30}•1CD.

Identification code	**NaP_5W_{30}•1CD**
Empirical formula	$C_{48}H_{55}K_{4.88}Na_6O_{185.25}P_5W_{30}$
Formula weight	9594.82
Temperature/K	200
Crystal system	Monoclinic
Space group	$P2_1$
***a*/Å**	40.522
***b*/Å**	20.995
***c*/Å**	25.108
***α*/ °**	90
***β*/ °**	98.55
***γ*/ °**	90
Volume/Å^3	21124.3
Z	4
ρ_{calc}g/cm^3	3.017
μ/mm^{-1}	16.521
F(000)	17114.0
Crystal size/mm^3	0.15 × 0.12 × 0.1
Radiation	MoKα (λ = 0.71073)
2Θ range for data collection/°	4.01 to 56.824
Index ranges	-54 ≤ h ≤ 54 -28 ≤ k ≤ 28 -33 ≤ l ≤ 33
Reflections collected	390618
Independent reflections	105407 R_{int} = 0.0726 R_{sigma} = 0.0603
Data/restraints/parameters	105407/62/2345
Goodness-of-fit on F^2	1.049
Final R indexes [I>=2σ (I)]	R_1 = 0.0490 wR_2 = 0.1182
Final R indexes [all data]	R_1 = 0.0546 wR_2 = 0.1228
Largest diff. peak/hole / e Å^{-3}	3.95/-3.76
Flack parameter	0.111(9)

3.2. Structural views of POM•1CD arrangement

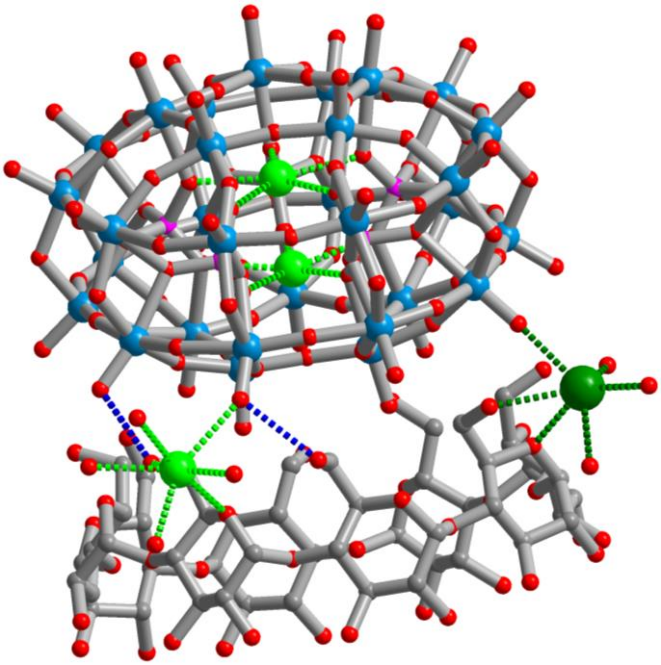

Figure S3. Structural representation of the **POM•1CD** arrangement showing the involvement of the potassium cations (dark-green spheres) and sodium cations (light-green spheres) within the POM•••γ-CD interactions in addition to the hydrogen bonds (dotted blue sticks).

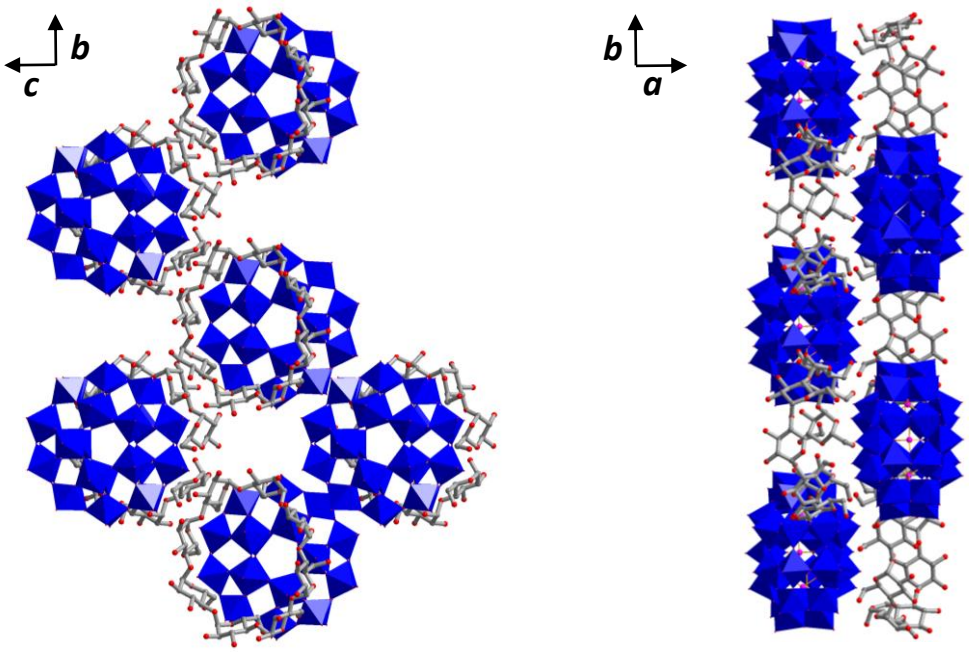

Figure S4. Representation of the **{NaP$_5$W$_{30}$}•1CD** structure showing chains of the POM and of the CD running along the *a* and *c* axes. The supramolecular host-guest assembly are alternately stacked through short and long intermolecular interactions involving the primary face of the γ-CD. These chains are mutually connected through the sodium/potassium counterions to give the monoclinic cell. Color code: blue polyhedral represent the W-O framework of the {NaP$_5$W$_{30}$}$^{14-}$ POM; the cyclodextrin are represented by grey sticks.

4. NMR data

4.1. ^{1}H NMR titration

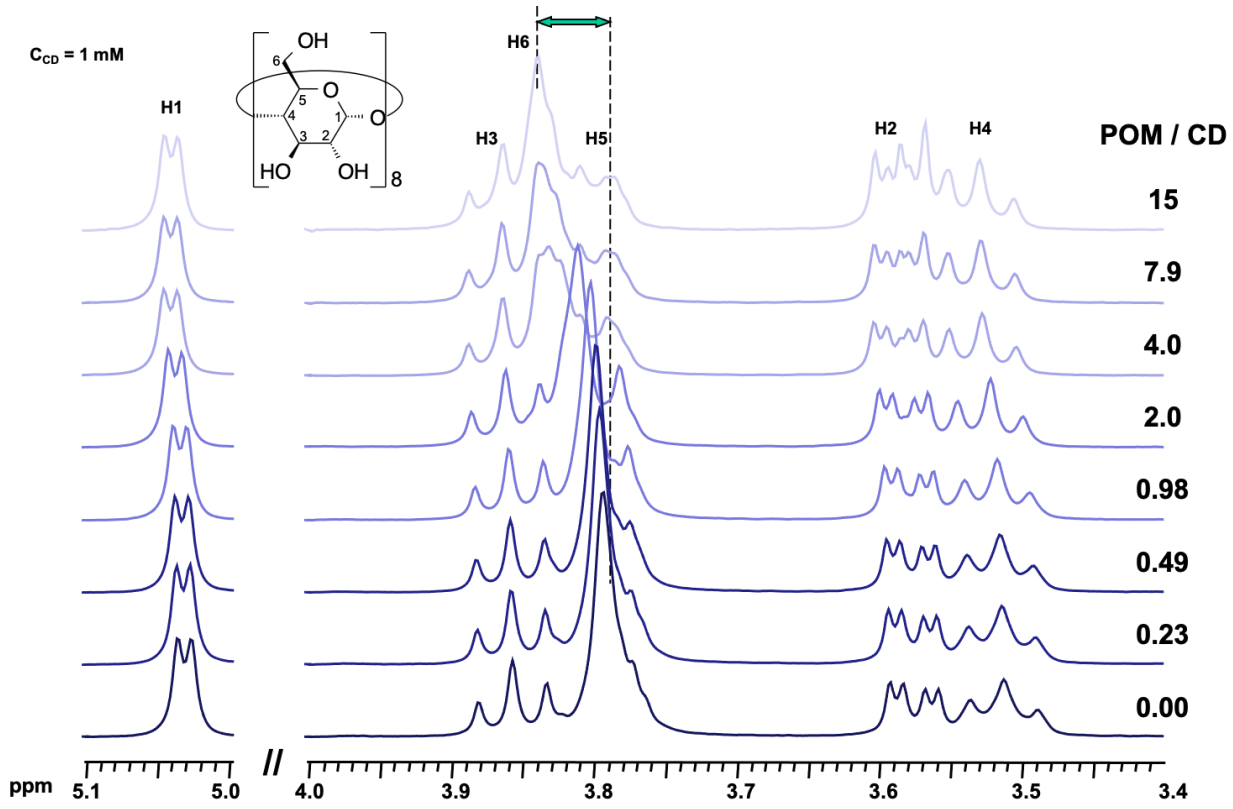

Figure S5. ^{1}H NMR spectra of γ-CD aqueous solution (3 mM) containing variable amounts of $K_{14}Na[P_5W_{30}O_{110}]$, showing effect on signal H_6 as a result of complex formation on the primary rim of the CD.

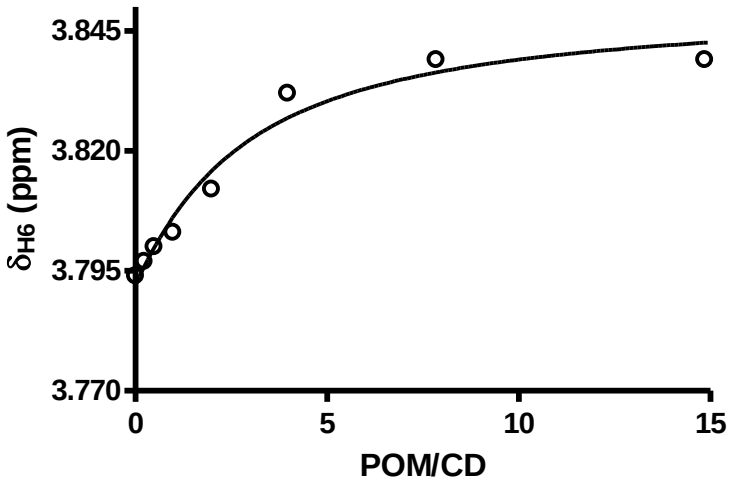

Figure S6. ^{1}H NMR titration curve of γ-CD with the POM. A plot of the chemical shifts of the higher field H6 proton of the γ-CD as a function of POM/CD molar ratio was used to estimate the association constant K (430 ± 60 M^{-1}) for the 1:1 complex.

4.2. ^{31}P NMR

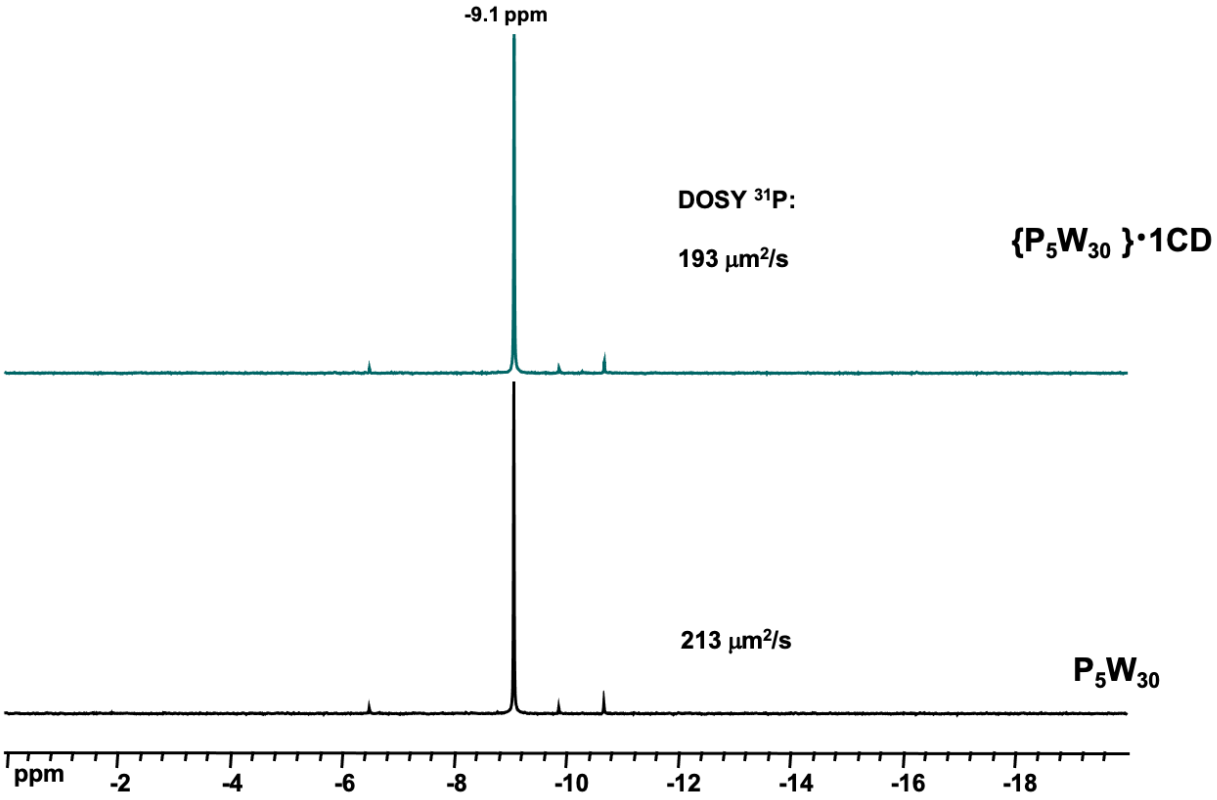

Figure S7. ^{31}P NMR spectra of $K_{14}Na[P_5W_{30}O_{110}]$ and **{NaP$_5$W$_{30}$}•1CD** aqueous solutions showing no effect on the POM signal.

5. Electrochemical impedance spectroscopy

5.1.Warburg coefficient

Short Warburg impedance $\mathbf{Z_w}$ is defined as:

$$\boldsymbol{Z_w} = \frac{\boldsymbol{\sigma_w}}{(\boldsymbol{i\omega})^{\boldsymbol{\beta}}}\tanh\left[(i\tau_w\omega)^{\beta}\right] \qquad \text{Eq. S1}$$

With ZView software, the same impedance is calculated using:

$$\boldsymbol{Z_w} = \frac{\boldsymbol{R_w}}{(\boldsymbol{i\tau_w\omega})^{\boldsymbol{\beta}}}\tanh\left[(i\tau_w\omega)^{\beta}\right] \qquad \text{Eq. S2}$$

By comparing Eq. S1 to Eq. S2, Warburg coefficient $\boldsymbol{\sigma_w}$ is deduced as follows:

$$\boldsymbol{\sigma_w} = \frac{\boldsymbol{R_w}}{(\boldsymbol{\tau_w})^{\boldsymbol{\beta}}} \qquad \text{Eq. S3}$$

Given the fact that $ß$ was also fitted for EIS data analysis, the comparison of $\mathbf{R_w}$ and $\boldsymbol{\tau_w}$ values cannot be justified.

5.2.EIS data

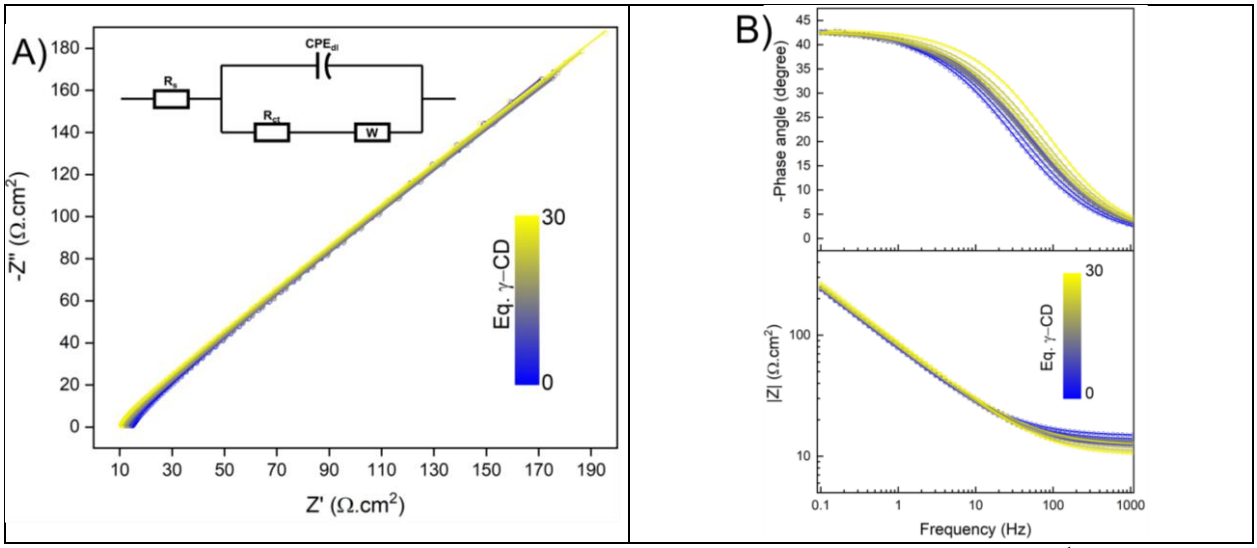

Figure S8. A) Nyquist diagram and B) Bode diagram of the $\mathbf{NaP_5W_{30}}$ anion (1 mmol.L^{-1}, glassy carbon working electrode) in the presence of increasing amounts of γ-CD (from 0 to 30 equivalents). The experiments have been performed at -0.43 V *vs* Ag/AgCl in 50:50 (v:v) HCl (0.1 mol.L^{-1}):NaCl (0.9 mol.L^{-1}) aqueous solution.

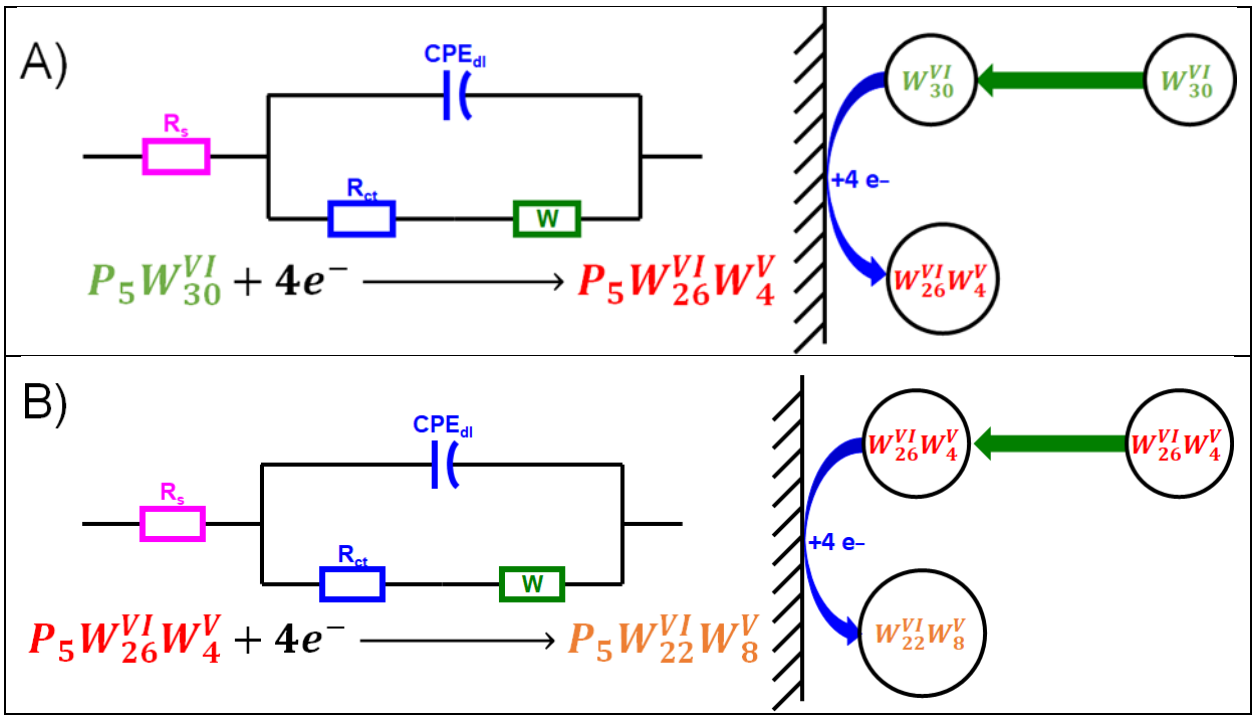

Figure S9. Correspondence of equivalent electric circuit to the proposed schematic mechanism of the electrochemical processes at A) -0.29 and B) -0.43V *vs* Ag/AgCl. (For better interpretation, the reader is referred to the online version).

Table S2. Electrochemical parameters calculated using ZView software for POM and POM–CD reduction reactions at A) -0.29 and B) -0.43 V *vs* Ag/AgCl.

A)	Eq. γ–CD	R_s (Ω.cm^2)	Q (mF.cm^{-2}.s$^{-α}$)	α	R_{ct} (Ω.cm^2)	R_w (Ω.cm^2.s$^{-ß}$)	τ_w (s)	ß
First cathodic peak	**0**	14.8	1.67	0.740	24.2	921	16.5	0.457
	0.5	13.7	1.32	0.761	18.3	883	16.8	0.460
	1	12.1	1.19	0.771	18.6	1844	79.7	0.468
	1.5	12.6	0.88	0.801	17.0	1871	81.8	0.475
	2	13.2	0.95	0.790	15.2	1831	81.0	0.472
	3	12.9	0.87	0.799	14.7	1753	72.0	0.473
	4	12.2	0.80	0.809	14.0	1786	75.8	0.476
	5	11.6	0.73	0.820	13.5	1794	75.5	0.478
	10	10.9	0.61	0.841	13.2	1788	67.7	0.482
	20	10.6	0.55	0.851	14.1	1793	65.4	0.483
	30	10.5	0.51	0.859	14.6	1833	59.6	0.486

B)	Eq. γ–CD	R_s (Ω.cm^2)	Q (mF.cm^{-2}.s$^{-α}$)	α	R_{ct} (Ω.cm^2)	R_w (Ω.cm^2.s$^{-ß}$)	τ_w (s)	ß
Second cathodic peak	**0**	14.7	2.03	0.737	30.5	1679	68.3	0.457
	0.5	13.6	1.84	0.742	26.3	1809	87.9	0.456
	1	12.0	1.59	0.759	20.8	1740	86.8	0.455
	1.5	12.6	1.57	0.756	21.2	1939	102.9	0.456
	2	13.1	1.56	0.754	20.0	1845	97.5	0.455
	3	12.8	1.60	0.749	21.9	1877	98.3	0.454
	4	12.2	1.53	0.753	20.7	1807	89.1	0.456
	5	11.5	1.41	0.762	18.5	1825	91.5	0.457
	10	10.8	1.24	0.775	16.0	1857	94.0	0.460
	20	10.4	1.11	0.786	15.7	1810	82.2	0.463
	30	10.2	0.97	0.800	14.8	1787	78.9	0.466